ELSEVIER

Thermochimica Acta 254 (1995) 277–304

thermochimica acta

Thermogravimetric kinetic study of the pyrolysis of municipal solid waste

A.N. García *, A. Marcilla, R. Font

Departamento de Ingeniería Química, Universidad de Alicante, Apartado 99, Alicante, Spain

Received 28 February 1994; accepted 14 July 1994

Abstract

A kinetic study of the pyrolysis of municipal solid waste (MSW) was carried out by thermogravimetric analysis (TGA). Different runs were performed at heating rates between 1.5 and 200°C min^{-1}. A correlation model that considers two independent reactions was applied to simulate the process. The values of the kinetic parameters were optimised and compared with the results obtained from the correlation of the experiments carried out in a Pyroprobe 1000, where the nominal heating rate was 20 000°C s^{-1}. In view of the results obtained, a theoretical analysis was developed with reference to the influence of the heating rate and the heat transfer on the kinetic parameters that can be obtained from the experimental data.

Keywords: DTG; Flash pyrolysis; Kinetics; Pyrolysis; TGA; Waste

List of symbols

a, a'	yield coefficients in kg of product formed per kg of reacted biomass
A	specific area of the sample to the heat transfer in m^2 kg^{-1}
b, b'	yield coefficient in kg of product formed per kg of reacted biomass
B	biomass at time t in kg
C	MSW cellulosic fraction in kg
$C_{p_{ash}}$	specific heat of MSW ash fraction in J kg^{-1} K^{-1}

* Corresponding author

SSDI 0040-6031(94)02002-7

C_{p_B} specific heat of MSW organic fraction at time t in J kg^{-1} K^{-1}
$C_{p_{B,0}}$ initial specific heat of MSW organic fraction in J kg^{-1} K^{-1}
$C_{p_{B,\infty}}$ final specific heat of MSW organic fraction at $t = \infty$ in J kg^{-1} K^{-1}
E_1 activation energy of the primary reaction in J mol^{-1}
$E_{1,C}$ activation energy of the primary reaction of the MSW cellulosic fraction in J mol^{-1}
$E_{1,NC}$ activation energy of the primary reaction of the MSW non-cellulosic fraction in J mol^{-1}
$E_{1,1}$ activation energy of the primary reaction of the decomposition process 1 in J mol^{-1}
$E_{1,2}$ activation energy of the primary reaction of the decomposition process 2 in J mol^{-1}
k_1 primary reaction rate constant in s^{-1}
$k_{1,1000\ K}$ primary reaction rate constant at 1000 K in s^{-1}
$k_{1,C}$ primary reaction rate constant of the decomposition of MSW cellulosic fraction in s^{-1}
$k_{1,C,1000\ K}$ primary reaction rate constant of the decomposition of MSW cellulosic fraction at 1000 K in s^{-1}
$k_{1,NC}$ primary reaction rate constant of the decomposition of MSW non-cellulosic fraction in s^{-1}
$k_{1,NC,1000\ K}$ primary reaction rate constant of the decomposition of MSW non-cellulosic fraction at 1000 K in s^{-1}
k_{01} pre-exponential factor of the primary rate constant in s^{-1}
$k_{01,C}$ pre-exponential factor of the primary rate constant of the MSW cellulosic fraction in s^{-1}
$k_{01,NC}$ pre-exponential factor of the primary rate constant of the MSW non-cellulosic fraction in s^{-1}
$k_{01,1}$ pre-exponential factor of the primary rate constant of the decomposition process 1 in s^{-1}
$k_{01,2}$ pre-exponential factor of the primary rate constant of the decomposition process 2 in s^{-1}
MSW municipal solid waste
NC MSW non-cellulosic fraction in kg
O.F. objective function
R universal gas constant in J mol^{-1} K^{-1}
R_1 residue generated at time t in kg
$R_{1,C}$ residue generated by the decomposition of the MSW cellulosic fraction at time t in kg
$R_{1,NC}$ residue generated by the decomposition of the MSW non-cellulosic fraction at time t in kg
t time in s
T absolute temperature of the sample in K
$T_{max,1}$ value of temperature at the peak maximum for the decomposition process 1 in °C

$T_{max,2}$ value of temperature at the peak maximum for the decomposition process 2 in °C
T_n nominal temperature in K
T_0 initial temperautre in K
T_t temperature read by the thermocouple placed at the bottom of the sample holder in K
U heat transfer coefficient in J s^{-1} m^{-2} K^{-1}
V_l volatiles generated at time t in kg
$V_{l,C}$ volatiles generated by the decomposition of the MSW cellulosic fraction at time t in kg
$V_{l,NC}$ volatiles generated by the decomposition of the MSW non-cellulosic fraction at time t in kg
V.C. variation coefficient in %
W mass fraction (biomass + residue) at time t
W_C cellulosic mass fraction (biomass + residue) at time t
$W_{C,0}$ initial cellulosic mass fraction
$W_{C,\infty}$ final cellulosic mass fraction (biomass + residue) at $t = \infty$
W_{cal} mass fraction calculated according to the model proposed at time t
W_{exp} experimental mass fraction at time t
W_{NC} non-cellulosic mass fraction (biomass + residue) at time t
$W_{NC,0}$ initial non-cellulosic mass fraction
$W_{NC,\infty}$ final non-cellulosic mass fraction (biomass + residue) at $t = \infty$
W_0 initial mass fraction
W_∞ final mass fraction (biomass + residue) at $t = \infty$
W_{ash} ash mass fraction
W_1 mass fraction which can be decomposed by process 1 at time t
$W_{1,0}$ initial mass fraction which can be decomposed by process 1
$W_{1,\infty}$ final mass fraction (biomass + residue) generated by process 1 at $t = \infty$
W_2 mass fraction which can be decomposed by process 2 at time t
$W_{2,0}$ initial mass fraction which can be decomposed by process 2
$W_{2,\infty}$ final mass fraction (biomass + residue) generated by process 2 at $t = \infty$
α extent of the reaction
α_{max} extent of the reaction at the peak maximum
β heating rate in °C s^{-1} or °C min^{-1}
$\bar{\varepsilon}_r$ relative error of the correlation in %

1. Introduction

Thermogravimetric analysis (TGA) is a useful technique for studying the decomposition reactions of a solid and it has been widely used to study the mechanisms and kinetics of the thermal decomposition of biomass. From the interpretation of isothermal as well as non-isothermal experiments, information can be obtained

about the composition of the biomass studied [1], reaction order [2], the number of different processes which take place and the kinetic constant values of the reactions [2–8].

According to Alves and Figueiredo [2], there are two possible explanations for the differences in kinetics found by researchers, even when a simple component, such as cellulose, is studied: (a) lack of attention paid to the internal and external heat transfer, which may lead to an important gap between the nominal and actual pyrolysis temperature, and (b) the use of simple models which may lead to kinetic parameters different from the real ones.

Different analyses of TGA data can be found in the literature: a widely used technique is a multi-heating-rate method proposed by Friedman, in which, the value of the activation energy can be obtained from the slope of the plot of the naperian logarithm of the mass loss (obtained at different heating rates) vs. the inverse of the absolute temperature at the same conversion values [1,9–12].

Another method to obtain the value of activation energy was calculated by Kissinger: this is based on the change in the position of the peak maxima, obtained at the temperature T_{max}, with the heating rate β used. From the linear regression of the $\ln(\beta/T_{max}^2)$ vs. $1/T_{max}$ plot, the activation energy can be calculated [13,14]. From a similar method calculated by Ozawa, the activation energy value can be obtained from the slope of the best fitting line by plotting $\log_{10}\beta$ vs. $1/T_{max}$ [15]. These methods are easy to use although, in general, it is difficult to locate the exact peak maxima positions and this would only be possible when: (a) a pure and homogeneous sample is treated, (b) the experiments are reproducible, and (c) only one process of decomposition takes place.

Cordero and co-workers [5,16] used a model to optimise the pre-exponential factor, activation energy and the breakpoint (the point where, according to the experimental TGA curve, one process seems to finish and another one begins) when two thermal processes are taken into account. The results obtained showed that the values of the kinetic parameters are independent of the heating rates. Varhegyi et al. [4] obtained similar conclusions by adjusting DTG data from the decomposition of cellulose, hemicellulose and sugar cane bagasse at 10 and 80°C min^{-1}.

However, emphasising the importance of the heat transfer, Bilbao et al. [7,8] drew attention to the influence of the moisture of the sample on the actual temperature and, consequently, on the kinetic constant as well as the increase in the difference between the actual and nominal temperature when the heating is high.

One of the limitations of TGA is the maximum heating rate that it can reach, which cannot be higher than 200°C min^{-1} (nominal heating rate). A Pyroprobe analytical apparatus can be used when studying pyrolysis of biomass at high heating rates [17–20].

In the present work, the thermal decomposition of municipal solid waste (MSW) in TGA has been studied. The following objectives have been proposed:

1. To obtain information about the processes of MSW thermal decomposition, at different heating rates using TGA.
2. To obtain the kinetic parameters of the primary reactions of MSW pyrolysis.

3. To compare the results obtained from TGA runs with those obtained at the highest heating rate in Pyroprobe 1000 experiments.

4. Theoretical analysis of the heating rate and heat transfer influences on the biomass decomposition in TG and Pyroprobe.

2. Experimental

The refuse used was MSW from a treatment plant in Alicante (Spain). The biomass was dried at 110°C for 12 h and kept in a desiccator until it was used. The weight percentage of moisture in the samples was in the range 1–1.5%. The initial sample weight was always within the range of 2.5–3.1 mg.

The equipment used to carry out the thermal decomposition of MSW was a Perkin-Elmer TGA7 thermobalance.

Ten dynamic (non-isothermal) runs were performed in an atmosphere of N_2 at different heating rates, 1.5, 20, 40, 80, 100 and 200°C min^{-1}. The weight loss vs. the temperature was plotted for each rate. The temperature was controlled by a thermocouple placed at the bottom of the sample holder, close to the sample. Therefore, although the thermocouple was not inside the sample, the values of the temperatures measured were assumed to be approximately the actual values.

The operating conditions were as follows: nitrogen flux, 66 ml min^{-1}; purge time, 60 min (to be sure the air was eliminated from the system and the atmosphere inert); initial temperature, 50°C; heating rate, 1.5–200°C min^{-1}; final temperature, 850°C.

At the end of each experiment, the nitrogen flux was replaced by an air flux and the residue was burnt at 900°C. In this way, the percentage of the ash in each

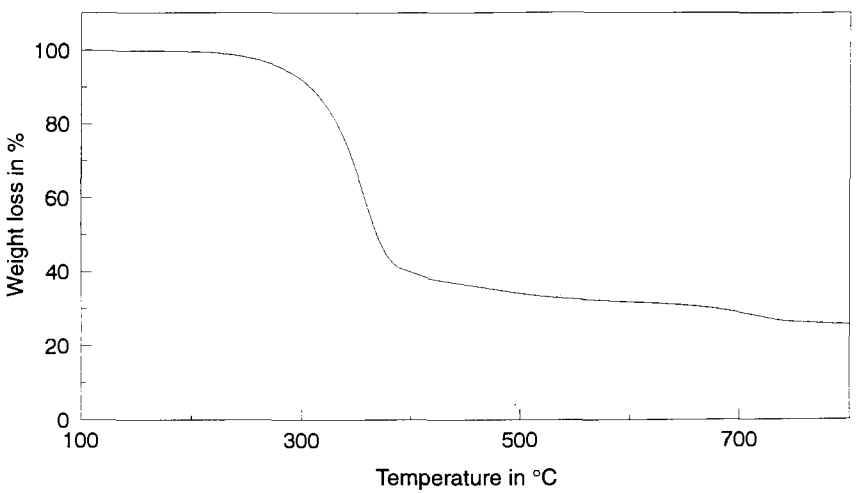

Fig. 1. Weight loss vs. temperature in dynamic TG (heating rate, 20°C min^{-1}).

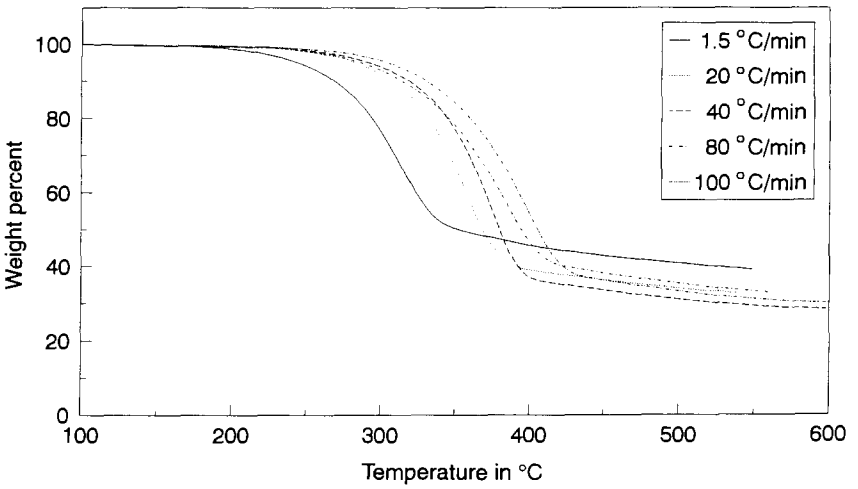

Fig. 2. Weight loss vs. temperature in dynamic TG runs at different heating rates.

sample was determined. Due to the small amount of sample used in each experiment and its heterogeneity, it is useful to know the percentage of ash when comparing the results.

3. Results and discussion

3.1. Thermal decomposition of MSW

Ten runs at six different nominal heating rates (1.5, 20, 40, 80, 100 and 200°C min^{-1}) were carried out. Fig. 1 shows the weight loss vs. temperature at 20°C min^{-1}. Similar curves were obtained for all the runs.

The experiments showed a weight loss of around 6.5–9.8% in a temperature range of 710–790°C. As the decomposition of the organic matter is normally total at these high temperatures, it was considered that this weight loss could be due to the decomposition of $CaCO_3$ present in the MSW ash. In order to prove this hypothesis, the residue obtained by thermal decomposition of MSW ($T_{initial} = 50°C$, $T_{final} = 475°C$, heating rate = 50°C min^{-1}, $t_{final} = 3$ min) was pyrolysed until 900°C in a TG with a mass spectrometer. (The sample was previously heated to 475°C, to avoid the system being obstructed by the tars generated in the pyrolysis of the raw sample.) This experiment revealed the CO_2 formation (around 750°C) and the CO formation (around 772°C). The quantification of these peaks was 5.2% for CO_2 and 2.0% for CO. If it is considered that around 80% of the CO obtained at this temperature was formed by the reaction $CO_2 + C \rightarrow 2CO$ [21], the initial CO_2 generated would be 6.5%, a value which agrees with the results obtained by TG, thus supporting the hypothesis that the reaction $CaCO_3 \rightarrow CaO + CO_2$ is taking

place. The mean value of the weight loss percentage due to $CaCO_3$ decomposition is 8.0%.

The MSW is a heterogeneous sample and this heterogeneity can be observed in the TG runs. Fig. 2 shows curves of weight loss vs. temperature at different heating rates. Two steps can be distinguished: a first step, where the most significant weight loss takes place; and a second step, at high temperatures, where the curves show abnormal crosses which are not experimentally reproduced, probably due to the sample heterogeneity and to the different percentage of components and ash of the samples. Similar results were found by Urban and Antal [10] when studying the thermal decomposition of sewage sludge (a heterogeneous material).

A shift in the curves of weight loss vs. temperature as a function of the heating rate has been described by different researchers [10,11,22–24]. These shifts could be a consequence of changes in the process mechanism when the heating rate varies. Furthermore, a slow heat transfer also increases the differences in the temperature of maximum weight loss rate (T_{max}) at different nominal heating rates as a consequence of the gap between the nominal and actual temperature. Independent of these causes, however, a real shift in T_{max} values is produced as a consequence of the influence of heating rate on the decompositon rate (even when extremely fast heat transfer takes place and the kinetic parameters are kept constant for the process). As demonstrated in previous papers [13,14], the peak maximum position can be expressed as a function of the heating rate. The influence of the activation energy and the pre-exponential factor of the process on the magnitude of the T_{max} (temperature corresponding to the peak) shift will be treated in this paper.

3.2. Kinetic models

In order to study the kinetics of the MSW decomposition process in this paper, data obtained at temperatures lower than 600°C were used because above this value the weight loss is due to the decomposition of the $CaCO_3$ present in the ash (see Section 3.1). Data above 600°C were treated, separately, in order to check if the kinetic parameters obtained from them are similar to those for $CaCO_3$ decomposition found in the literature.

In view of the experimental curves obtained, a first kinetic model was considered in which the weight loss was associated with *a single process of decomposition*, according to the reaction

$$B \rightarrow aR_1 + bV_1 \tag{1}$$

where B is the biomass, R_1 the residue and V_1 the volatiles generated at time t. The yield coefficients a and b are expressed as grams of R_1 or V_1 divided by grams of reacted biomass $(B_0 - B)$ at infinite time, where B_0 is the initial biomass.

Considering the fraction of solids W (sum of the non-reacted biomass and the residue formed) and a primary order reaction for the decomposition, it can be written that

$$\frac{dW}{dt} = -k_1(W - W_\infty) \tag{2}$$

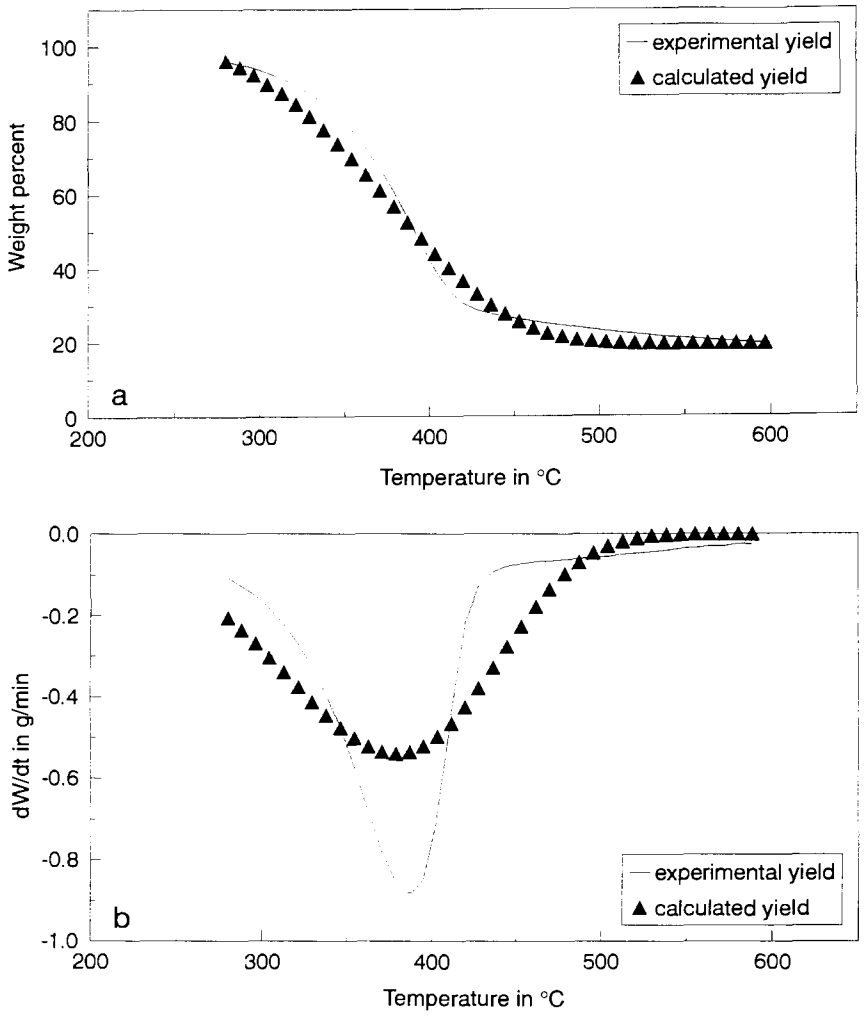

Fig. 3. Experimental and calculated TG (a) and DTG (b) curves according to the model that considers a single reaction. Heating rate, 100°C min^{-1}.

where k is the kinetic constant of the process and W_∞ is the final fraction of solid residue obtained at 600°C, where $CaCO_3$ was not decomposed.

Expressing the kinetic constant by an Arrhenius equation, Eq. (2) can be written as

$$\frac{dW}{dt} = -k_{01} \exp(-E_1/RT_t)(W - W_\infty) \tag{3}$$

where k_{01} and E_1 are the pre-exponential factor and the activation energy, respectively. The temperature values considered (T_t) were those read by the thermocouple placed at the bottom of the sample holder.

Eq. (3) has been numerically integrated by a fourth-order Runge–Kutta method. A calculation program (Flexible Simplex Method) [25] was elaborated to optimise the kinetic parameters k_{01} and E_1.

Due to the interrelation between the pre-exponential factor and the activation energy, Eq. (3) has been replaced by another one expressed as a function of a kinetic constant at a fixed temperature (1000 K in this case)

$$\frac{dW}{dt} = k_{1,1000\,K} \exp[-(E_1/R)(1/T_t - 1/1000)](W - W_\infty) \quad (4)$$

The optimised parameters were the activation energy and the kinetic constant at 1000 K. The objective function (O.F.) considered was

$$\text{O.F.} = \sum [(W_{cal} - W_{exp})^2/(W_{cal} + W_{exp})^2] \quad (5)$$

where the subscripts cal and exp indicate calculated values (by the model proposed) and experimental values (from the TG curve), respectively.

The results obtained were $k_{1,1000\,K} = 0.651\ s^{-1}$ and $E_1/R = 6123$ K.

Fig. 3 shows the experimental and calculated curves (TG and DTG) at 100°C min^{-1}. From Fig. 3, it can be deduced that the model proposed (with a single decomposition process) is not adequate for simulating the degradation of MSW. This is logical because MSW is a multi-component sample.

Agrawal [1] performed some TG studies on some pure components of MSW and their mixtures. According to Agrawal, the pyrolysis of several cellulosic wastes takes place in the same range of temperature with similar kinetic constants. Consequently, in a process of thermal conversion, the cellulosic fraction of MSW does not need to be characterised in its individual components: paper, feed refuses, agricultural refuses, textiles, etc., because all of these generate similar yields of products and are chemically similar. The temperature range of cellulose decomposition is 300–400°C (when the heating rate is 5°C min^{-1}). When the cellulosic refuse has a high percentage of impurities such as ash and lignin, e.g. newsprint or kraft paper, the reaction temperature is in the range 250–375°C. Similar results were shown by Helt et al. [26]. However, the depolymerisation of plastics takes place at higher temperatures than cellulosic refuse decomposition (400–470°C for polystyrene and 400–500°C for polyethylene). The pyrolysis of newsprint and polyethylene mixtures shows the presence of two processes (around 360 and 425°C respectively, when the heating rate is 5°C min^{-1}); the second one increases when the plastic percentage in the mixture is increased [1].

In accordance with the experimental data shown in Fig. 3 and taking into account the heterogeneity of MSW and the previous comments, two different processes of decomposition are necessary to try to simulate the overall process: (a) a cellulosic fraction decomposition, and (b) other organic refuses which decompose in a wider range of temperature than the cellulosic fraction. A second model was therefore proposed where the *decomposition of two independent fractions* was considered: the cellulosic fraction (C) and the non-cellulosic fraction, plastics and other refuses (NC)

$$C \rightarrow aR_{1,C} + bV_{1,C} \quad (6)$$

$$NC \rightarrow a'R_{1,NC} + b'V_{1,NC} \quad (7)$$

where $R_{1,i}$ is the residue and $V_{1,i}$ the volatiles generated by the fraction i at time t. The coefficients a, a' and b, b' are expressed as grams of $R_{1,i}$ or $V_{1,i}$ divided by grams of C or NC decomposed.

A similar scheme was proposed by Varhegyi et al. [4] when studying the decomposition of lignocellulosic refuses and by Font et al. [3] in the kinetic study of almond shell decomposition, where two processes also apparently take place.

As in the previous case, considering a primary order reaction

$$\frac{dW_C}{dt} = -k_{1,C}(W_C - W_{C,\infty}) \quad (8)$$

$$\frac{dW_{NC}}{dt} = -k_{1,NC}(W_{NC} - W_{NC,\infty}) \quad (9)$$

Table 1
Kinetic constants, activation energy values and fitting parameters of the MSW thermal decomposition

Heating rate in °C min^{-1}	$k_{1,C,1000\,K}$ in s^{-1} $k_{1,NC,1000\,K}$ in s^{-1}	$E_{1,C}/R$ in K $E_{1,NC}/R$ in K	$W'_{C,0} - W'_{C,\infty}$ [a] $W'_{NC,0} - W'_{NC,\infty}$ [a]	O.F.	$\bar{\varepsilon}_r$ in %
1.5	222.4	17526	0.552	1.51 E − 3	0.9
	7.55 E − 4	2076	0.198		
20	189.3	15631	0.465	1.569 E − 3	1.0
	0.012	2880	0.318		
20	271.2	17013	0.613	1.790 E − 3	1.1
	0.020	3712	0.191		
40	204.0	16424	0.634	3.671 E − 3	1.5
	0.031	4019	0.162		
40	256.4	17235	0.517	2.321 E − 3	1.1
	0.024	3317	0.236		
80	192.5	15801	0.549	1.786 E − 3	1.6
	0.058	3089	0.227		
80	229.2	16219	0.487	1.482 E − 3	0.9
	0.049	3146	0.309		
100	237.5	16737	0.568	2.153 E − 3	1.1
	0.076	3748	0.238		
100	245.1	16430	0.554	1.015 E − 3	0.8
	0.062	3239	0.258		
200	209.1	14732	0.483	1.983 E − 3	1.2
	0.11	3243	0.281		
$\bar{X}$	225.7	16375	0.542	–	–
	0.045	3229	0.242		
V.C. in % [b]	12	5	10	–	–
	75	17	21		

[a] $(W'_{C,0} - W'_{C,\infty})$ and $(W'_{NC,0} - W'_{NC,\infty})$ are expected on an ash-free basis. [b] Variation coefficient.

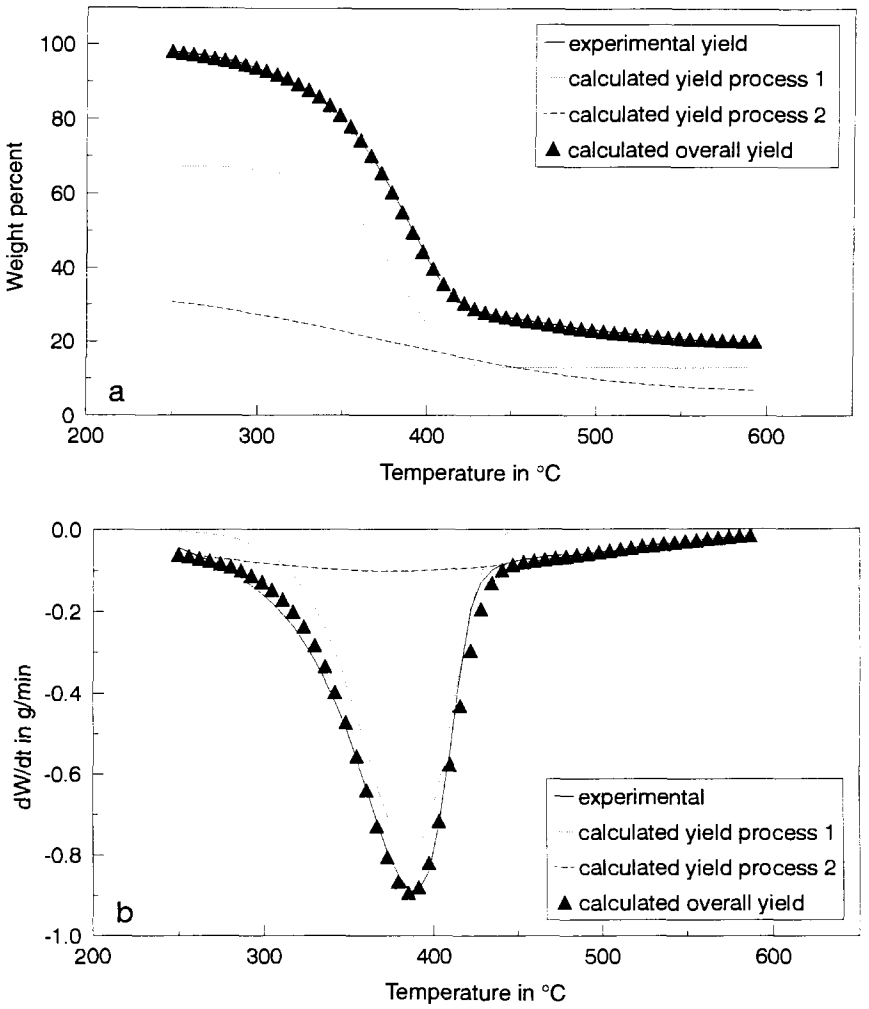

Fig. 4. Experimental and calculated TG (a) and DTG (b) curves according to the model that considers two independent reactions. Heating rate 100°C min^{-1}.

where $k_{1,C}$ and $k_{1,NC}$ are the kinetic constants of the processes, and $W_{C,\infty}$ and $W_{NC,\infty}$ are the final fractions of solid residue obtained in the two fractions considered, respectively.

Following a similar discussion of the previous model and, taking into account that, in this case, two independent fractions undergo decomposition, the expression can be obtained

$$\frac{dW_i}{dt} = k_{1,i,1000\,K} \exp[-(E_{1,i}/R)(1/T_t - 1/1000)](W_i - W_{i,\infty}) \quad (10)$$

where $k_{1,i,1000\,K}$ and $E_{l,i}$ are the kinetic constant of the decomposition process of the fraction i and the activation energy respectively, $i = C, NC$.

Obviously

$$W_\infty = W_{C,\infty} + W_{NC,\infty} \tag{11}$$

$$W_0 = W_{C,0} + W_{NC,0} = 1 \tag{12}$$

Eq. (10), together with Eqs. (11) and (12), were numerically integrated by a fourth-order Runge–Kutta method.

The optimised parameters (using a Flexible Simplex Method) were: the activation energies of both processes ($E_{1,C}$ and $E_{1,NC}$), kinetic constants at 1000 K of both reactions ($k_{1,C,1000\,K}$ and $k_{1,NC,1000\,K}$) and the value ($W_{C,0} - W_{C,\infty}$). Although W_∞ and W_0 are known, only one of the variables $W_{C,0} - W_{C,\infty}$ or $W_{NC,0} - W_{NC,\infty}$ can be considered as a parameter of optimisation. The other variable $W_{i,0} - W_{i,\infty}$ is deduced from the variable known, but the determination of $W_{C,0}$, $W_{NC,0}$, $W_{C,\infty}$ and $W_{NC,\infty}$ is not possible. In order to obtain these results, the experimental weight loss data (W_{exp}), the measured temperature (T_t) values, and W_0 and W_∞ data were considered.

The objective function O.F. to be minimised, in this case, was

$$\text{O.F.} = \sum [((W_C + W_{NC})_{cal} - (W_C + W_{NC})_{exp})^2 / ((W_C + W_{NC})_{cal} + (W_C + W_{NC})_{exp})^2] \tag{13}$$

where the subscripts cal and exp indicate calculated values (by the model proposed) and experimental data (from TG curve), respectively.

Table 1 shows the value of the parameters obtained for each fitting, as well as the value ($W_{NC,0} - W_{NC,\infty}$) calculated as $((W_{NC,0} + W_{C,0}) - (W_{C,\infty} + W_{NC,\infty}) - (W_{C,0} - W_{C,\infty}))$. The values of the O.F. obtained and the mean relative error $\bar{\varepsilon}_r$, defined as follows, are also shown

$$\bar{\varepsilon}_r = \sqrt{\frac{4(\text{O.F.})}{n \text{ points}}} \tag{14}$$

Fig. 4 shows the experimental curves (TG and DTG) for the thermal decomposition of MSW at 100°C min^{-1}, as well as the theoretical curves obtained, according to the model proposed for the decomposition of the cellulosic and non-cellulosic fractions. It can be observed that the non-cellulosic fraction includes all the components which decompose in a wide range of temperature. Fig. 4 also shows good agreement between the experimental curves and those calculated according to the model proposed.

From the values shown in Table 1, it cannot be concluded that a significant difference between the kinetic parameters obtained as a function of the heating rate exists. The dispersion of the results is higher for the kinetic constants referring to the non-cellulosic fraction because it is more heterogeneous than the cellulosic fraction. This heterogeneity makes it difficult to fit all the runs simultaneously, as the percentage of the cellulosic and non-cellulosic fraction varies from one sample to another.

A third model was elaborated to try to determine if the cause of dispersion in the results was simply the heterogeneity of the sample or a poor heat transfer which could influence the results. This model includes the *heat transfer effect*. Two new expressions were considered

$$\frac{dT}{dt} = U\frac{(W_{ash} + W_C + W_{NC})A}{(W_{ash}C_{p_{ash}} + (W_C + W_{NC})C_{p_B})}(T_t - T) \tag{15}$$

and

$$C_{p_B} = \left(\frac{C_{p_{B,\infty}} - C_{p_{B,0}}}{(W_C + W_{NC})_\infty - (W_C + W_{NC})_0}\right)((W_C + W_{NC}) - (W_C + W_{NC})_0) + C_{p_{B,0}} \tag{16}$$

where U is the heat transfer coefficient (J s^{-1} m^{-2} K^{-1}), W_{ash} the mass fraction of ash in the sample, A the specific area of the sample to the heat transfer (m^2 kg^{-1}), C_{p_B} the organic fraction heat capacity at time t (J kg^{-1} K^{-1}), and $C_{p_{ash}}$ the ash heat capacity. The mean value considered was 850 J kg^{-1} K^{-1} for the inorganic components. This is the value given by Perry and Chilton [27] for the heat capacity of stones. $C_{p_{B,0}}$ is the initial organic fraction heat capacity; the mean value considered was the cellulose heat capacity (1338 J kg^{-1} K^{-1}). $C_{p_{B,\infty}}$ is the final organic fraction heat capacity; the mean value considered was the charcoal heat capacity (1012 J kg^{-1} K^{-1}). T_t is the temperature (K) read by the thermocouple placed at the bottom of the sample holder.

The reason for considering different heat capacities for the organic fraction and the ash is the influence of the inorganic material tested experimentally in mixtures with polymers. A shift of the TG curve to low temperatures was observed when the sand percentage was increased in a sand and polyethylene mixture. Similar considerations were presented by Biader Ceipidor et al. [28], when taking into account the differences between the sample holder and the sample heat capacities, bearing in mind that the sample heat capacity is that of a mixture of reactant and product.

Eq. (15) was numerically integrated together with Eq. (10) by the Runge–Kutta algorithm. Seven parameters were optimised in this case: the five previous parameters, the specific area of the sample to the heat transfer (A) and the heat transfer coefficient (U). The results obtained were similar to those found with the previous model, where the heat transfer coefficient was not included. Similar dispersion of the results was obtained in this case.

Note that the temperature used in the model was not the nominal temperature (heating rate × time) but the temperature registered by the thermocouple. Furthermore, the sample amount used was always small (2.5–3.1 mg) and the moisture was around 1% in all cases. Due to this, the difference $(T_t - T)$ (Eq. (15)) has a low value and the term dT/dt has no significant value in the final result. It appears that the dispersion of the results is mainly due to the heterogeneity of the sample.

The Kissinger method was used to estimate the activation energy of the cellulosic fraction decomposition (due to the shape of the curve, determination of the position of the peak of the second process was not possible). From the linear

regression of the $\ln(\beta/T_{max}^2)$ vs. $1/T_{max}$ curve, the E/R value obtained was 15 932 K which is very close to the mean value obtained by the Flexible Simplex Method ($E/R = 16\,375$ K). In the Kissinger plotting, the independent term b is equal to $\ln[-k_0 R f'(\alpha_{max})/E]$ (where α_{max} is the extension of the reaction at the peak maximum decomposition rate and $f(\alpha)$ is the function of the extension α of the reaction). When a first-order reaction is considered, $f(\alpha) = 1 - \alpha$; therefore, $b = \ln[k_0 R/E]$. In this case, from the linear regression performed, the value of the k_0 calculated is 1.70×10^9 s^{-1}, which is very close to the value obtained by the flexible simplex method ($k_0 = 2.92 \times 10^9$ s^{-1}). Despite the heterogeneity of the sample and the different processes which take place that cannot be detected by the Kissinger method, the activation energy value calculated by this method is in good agreement with the value obtained for the majority decomposition process of MSW according to the optimisation method proposed.

The Kissinger method was also used to calculate the kinetic parameters of the decomposition which takes place at above 600°C. The E/R and k_0 values obtained were 24 413 K and 5.8×10^8 s^{-1}, respectively. Data found in the literature for the $CaCO_3$ decomposition show an E/R value around 24 000 K and a k_0 value depending on the particle size: for example, around 2.3×10^{10} s^{-1} when the particle diameter is 1 μm and around 3.4×10^8 s^{-1} when it is 90 μm [29]. A good agreement between the results presented in this paper and those found in the literature may be observed. This could be considered as further proof of the fact that the weight loss above 600°C is due to the $CaCO_3$ decomposition.

Kinetic parameter values for the MSW decomposition have not been found in the literature. However, as the first process considered probably corresponds to the cellulosic fraction decomposition, it could be compared with kinetic data for

Table 2
Arrhenius parameters for the decomposition of some cellulosic refuses

Author	Sample	k_0 in s^{-1}	E in kJ mol^{-1}	$k_{673\,K}$ in s^{-1}
[30]	Modified cellulose	1.66×10^{10}	133.8	0.684
[31]	Cellulose	7.00×10^9	153.0	0.00932
[2]	Whatman filter	1.13×10^{11}	167.2	0.0119
[7]	Cellulose	5.00×10^{17}	227.0	1.202
[6]	Cellulose	4.70×10^{12}	182.7	0.0310
[4]	Cellulose	3.98×10^{17}	234.0	0.274
[1]	Whatman filter	1.53×10^{14}	204.8	0.0194
[1]	Newsprint	1.67×10^{12}	109.9	0.00493
[1]	Kraft paper	2.83×10^{11}	168.9	0.0220
Present paper	MSW cellulosic fraction	2.92×10^9	135.9	0.0826

Table 3
Kinetic parameters obtained from TG and Pyroprobe 1000

Experimental technique	k_{01} in s^{-1}	E_1 in kJ mol^{-1}	$k_{673\,K}$ in s^{-1}
TG	2.92×10^9	135.9	0.0826
(heating rate range: 1.5–200°C min^{-1}) (2 processes)	1.13	26.8	0.0094
(good correlation)			
TG	297.0	50.8	0.0339
(heating rate range: 1.5–200°C min^{-1}) (1 process)			
(bad correlation)			
Pyroprobe 1000	2214	44.8	0.7378
(nominal heating rate: 20 000°C s^{-1}) (1 process)			
(good correlation)			

pyrolysis of cellulosic refuses, shown in Table 2. It can be deduced that the activation energy value obtained in this paper is closer to the values found in the literature for the decomposition of modified cellulose than to those for pure cellulose. The value obtained is also within the range of the values found for the decomposition of newsprint and kraft paper presented by Agrawal [1]. These facts are logical, because the cellulosic fraction of the MSW is formed by these components in a degraded stage.

3.3. Comparison between kinetic parameters obtained from TG and the Pyroprobe 1000

The flash pyrolysis of MSW at different temperatures (500–900°C) in a Pyroprobe 1000 has been studied previously [19]. The nominal heating rate used was 20 000°C s^{-1}. A model which considered the kinetic law and the heat transfer in the heating as well as in the sample cooling step was developed to study the kinetics of the MSW decomposition. According to this model, the actual heating rate was in the range 250–585°C s^{-1}. The kinetic parameters obtained are shown in Table 3.

The information obtained from the correlation of TG data is different from the results obtained in the Pyroprobe 1000. While in the first case, two different reactions must be considered in order to obtain a good correlation of the experimental data, this is not necessary in the second case, where a model with a single reaction is sufficient to reproduce the experimental data.

Table 3 compares the kinetic parameters obtained in the TG and Pyroprobe. In view of these results a theoretical analysis was developed showing the influence of the heating rate on the kinetic results that can be obtained from the experimental data. The following aspects were considered:

1. Why some processes seem to be formed by a single or several reactions, depending on the heating rate.
2. What occurs when two independent reactions are correlated according to a model which considers a single reaction.

Table 4
Shift of the TG curve vs. the heating rate, activation energy and pre-exponential factor

	Heating rate in °C s^{-1}	k_0 in s^{-1}	E/R in K	T_{max} in K	$T - T_{10-6\,°C\,s^{-1}}$ in K
	10^{-1}	2.439×10^4	9638.6	600	237
A	10^{-3}	2.439×10^4	9638.6	478	115
	10^{-6}	2.439×10^4	9638.6	363	0
	10^{-1}	2.439×10^4	38554.2	2228	843
B	10^{-3}	2.439×10^4	38554.2	1798	413
	10^{-6}	2.439×10^4	38554.2	1385	0
	10^{-1}	7.422×10^{25}	38554.2	602	90
C	10^{-3}	7.422×10^{25}	38554.2	562	50
	10^{-6}	7.422×10^{25}	38554.2	512	0
	10^{-1}	7.422×10^{25}	9638.6	153.5	23
D	10^{-3}	7.422×10^{25}	9638.6	143.5	13
	10^{-6}	7.422×10^{25}	9638.6	130.5	0

The answers to these questions are discussed in the following sections.

3.3.1. Heating rate influence on the decomposition temperature of biomass

As explained in Section 3.1, the decomposition range of temperatures depends on the heating rate [13,14,23]. Different theoretical TG curves corresponding to a first-order reaction were simulated to determine the influence of the activation energy and the pre-exponential factor values in the shift in the decomposition range.

The expressions used were

$$\frac{dW}{dt} = -k_0 \exp(-E/RT)(W - W_\infty) \tag{17}$$

$$T = T_0 + \beta t \tag{18}$$

where W is the mass fraction of biomass at time t, W_∞ the mass fraction of biomass at time infinity, k_0 the pre-exponential factor (s^{-1}), E the activation energy (J mol^{-1} K^{-1}), R the universal gas constant (J mol^{-1} K^{-1}), T the absolute temperature (K), T_0 the initial temperature (323 K), β the heating rate (°C s^{-1}), and t the reaction time (s).

Eq. (17) was numerically integrated by a fourth-order Runge–Kutta algorithm. A theoretical curve of weight loss vs. T is obtained when E, k_0 and β are fixed. Table 4 shows the values of the temperature (T_{max}) of maximum weight loss rate and the shift of the peak (in units of temperature) at different heating rates for four different processes. The magnitudes of these shifts are functions of the activation energy and pre-exponential factor values: when the pre-exponential factor is constant, the higher the activation energy, and the process is more sensitive to the heating rate; when the activation energy is constant, the lower the pre-exponential

factor, and the process is more sensitive to the heating rate. That means that a process with a high pre-exponential factor value and a low activation energy value would show small differences between the T_{max} obtained when the heating rates are modified. It is possible to obtain the same result by increasing the pre-exponential factor and decreasing the activation energy. Comparing the values of only one of these parameters, without bearing the other value in mind, can lead to wrong conclusions.

Flynn [32,33] studied the effect of the heating rate on the coupling of complex reactions and some similar aspects considered in this paper seem to be present. Flynn represented the theoretical curves for four independent first-order reactions with the kinetic parameters: $k_{0,1} = 2.139 \times 10^4$ s^{-1} and $E_1 = 80$ kJ mol^{-1}, $k_{0,2} = 4.457 \times 10^{11}$ s^{-1} and $E_2 = 160$ kJ mol^{-1}, $k_{0,3} = 6.104 \times 10^{18}$ s^{-1} and $E_3 = 240$ kJ mol^{-1}, $k_{0,4} = 7.422 \times 10^{25}$ s^{-1} and $E_4 = 320$ kJ mol^{-1}, and at eleven heating rates between 10^4 and 10^{-6}°C s^{-1}. His results showed a shift of the curves to higher temperatures when the heating rate is increased and the magnitude of this shift is decreased from process 1 to process 4. According to Flynn, the cause of these results is the fact that process 1 has the lowest value of E and process 4 has the highest value of E, deducing that the magnitude of the shift is inversely proportional to the activation energy value. Nevertheless, if the differences between the pre-exponential factor values of the processes are taken into account, different conclusions could be obtained.

The interesting idea exposed by Flynn can be checked and completed using the previous simulation model of theoretical curves of TG: cases A and C in Table 4 reproduce two processes studied by Flynn at three heating rates and the T_{max} values obtained agree perfectly with those deduced from the graphs presented in his papers. The values of k_0 and E of these processes have been exchanged in cases B

Table 5
Real process: 2 independent reactions and extremely rapid heat transfer

$k_{01,1}$ in s^{-1}	$E_{1,1}$ in kJ mol^{-1}	$T_{max,1}$ in °C	$k_{01,2}$ in s^{-1}	$E_{1,2}$ in kJ mol^{-1}	$T_{max,2}$ in °C	Heating rate in °C s^{-1}
5×10^7	112.0	345	5×10^{17}	242.1	375	0.25
5×10^7	112.0	395	5×10^{17}	242.1	395	1
5×10^7	112.0	510	5×10^{17}	242.1	475	100
5×10^7	112.0	640	5×10^{17}	242.1	520	1000

Correlation model: 1 single reaction and extremely rapid heat transfer

k_{01} in s^{-1}	E_1 in kJ mol^{-1}	T_{max} in °C	$k_{1000\ K}$ in s^{-1}	Heating rate in °C s^{-1}
1.3×10^7	111.0	360	20.1	0.25
1.4×10^{10}	145.3	385	353.4	1
1.9×10^6	88.0	490	48.0	100
2.2×10^4	53.1	550	37.0	1000

and D. Comparing cases A and C, case A, which has the lowest activation energy value, undergoes the highest shift when the heating rate is increased, and similarly for case B when it is compared with case D, although here B is the process which has the highest value of E. Therefore, if Flynn had considered cases B and D instead of cases A and C, he would have obtained the opposite conclusion.

In accordance with the previous comments, it can be understood why two independent processes, which take place at different temperature ranges when a low heating rate is used, can be superposed, or the order of appearance even reversed, when the heating rate is sufficiently increased. This fact occurs in a case with the following characteristics: (a) the activation energy of process 1 is less than that of process 2; (b) at low heating rates, reaction 1 takes place at lower temperatures than reaction 2; and (c) the pre-exponential factor of reaction 1 is less than that of process 2. Under these assumptions, process 1, which takes place at lower temperatures at low heating rates, is more sensitive to the heating rate than process 2 which takes place at higher temperatures at low heating rates. When the heating rate is increased, process 1 undergoes a bigger shift than process 2, and process 1 can therefore take place at the same temperature as process 2 or even at a higher temperature if the heating rate is sufficiently high. These characteristics can be observed in cases A, B, C and D in Table 4.

3.3.2. A single reaction model to correlate a process of two reactions

As can be deduced from the results presented in this paper, the interpretation of the experimental data depends on factors such as the heating rate, the heat transfer process, etc., and all these factors must be considered to avoid significant errors.

This section illustrates the error produced when a process of two reactions is correlated by a single reaction model (such as in the pyrolysis of MSW and a wide

Table 6
Real process: 2 independent reactions and extremely rapid heat transfer

$k_{01,1}$ in s^{-1}	$E_{1,1}$ in kJ mol^{-1}	$T_{max,1}$ in °C	$k_{01,2}$ in s^{-1}	$E_{1,2}$ in kJ mol^{-1}	$T_{max,2}$ in °C	Heating rate in °C s^{-1}
5×10^7	112.0	345	5×10^{17}	242.1	375	0.25
5×10^7	112.0	395	5×10^{17}	242.1	395	1
5×10^7	112.0	510	5×10^{17}	242.1	475	100
5×10^7	112.0	640	5×10^{17}	242.1	520	1000

Correlation model: 1 single reaction with heat transfer parameter

k_{01} in s^{-1}	E_1 in kJ mol^{-1}	T_{max} in °C	$k_{1000\,K}$ in s^{-1}	U in J s^{-1} m^{-2} K^{-1}	Heating rate in °C s^{-1}
1.2×10^7	110.5	360	19.7	260	0.25
9.6×10^9	143.2	385	310.9	542	1
9.7×10^5	83.0	490	44.0	24000	100
2.1×10^4	52.6	550	37.0	98000	1000

Table 7
Real process: 2 independent reactions and fast heat transfer

$k_{01,1}$ in s^{-1}	$E_{1,1}$ in kJ mol^{-1}	$T_{max,1,real}$ in °C	$T_{max,1,nominal}$ in °C	$k_{01,2}$ in s^{-1}	$E_{1,2}$ in kJ mol^{-1}	$T_{max,2,real}$ in °C	$T_{max,2,nominal}$ in °C	U in J s^{-1} m^{-2} K^{-1}	Heating rate in °C s^{-1}
5×10^7	112.0	345	345	5×10^{17}	242.1	375	375	300	0.25
5×10^7	112.0	395	395	5×10^{17}	242.1	395	395	300	1
5×10^7	112.0	535	535	5×10^{17}	242.1	480	560	300	100
5×10^7	112.0	680	1240	5×10^{17}	242.1	520	1150	300	1000

Correlation model: 1 single reaction with heat transfer parameter

k_{01} in s^{-1}	E_1 in kJ mol^{-1}	$T_{max,real}$ in °C	$T_{max,nominal}$ in °C	$k_{1000\ K}$ in s^{-1}	U in J s^{-1} m^{-2} K^{-1}	Heating rate in °C s^{-1}
1.1×10^7	110.2	360	360	19.3	96	0.25
2.2×10^{10}	147.8	385	385	412.7	3581	1
5.4×10^7	116.2	555	570	44.8	1456	100
3.1×10^4	58.1	660	1205	28.4	417	1000

Table 8
Real process: 2 independent reactions and slow heat transfer

$k_{01,1}$ in s^{-1}	$E_{1,1}$ in kJ mol^{-1}	$T_{max,1,real}$ in °C	$T_{max,1,nominal}$ in °C	$k_{01,2}$ in s^{-1}	$E_{1,2}$ in kJ mol^{-1}	$T_{max,2,real}$ in °C	$T_{max,2,nominal}$ in °C	U in J s^{-1} m^{-2} K^{-1}	Heating rate in °C s^{-1}
5×10^7	112.0	345	345	5×10^{17}	242.1	375	375	80	0.25
5×10^7	112.0	395	395	5×10^{17}	242.1	395	395	80	1
5×10^7	112.0	560	805	5×10^{17}	242.1	480	770	80	100
5×10^7	112.0	660	2090	5×10^{17}	242.1	510	1960	80	1000

Correlation model: 1 single reaction with heat transfer parameter

k_{01} in s^{-1}	E_1 in kJ mol^{-1}	$T_{max,real}$ in °C	$T_{max,nominal}$ in °C	$k_{1000\,K}$ in s^{-1}	U in J s^{-1} m^{-2} K^{-1}	Heating rate in °C s^{-1}
1.5×10^7	111.9	360	360	21.4	658	0.25
4.8×10^{10}	152.2	385	385	521.4	6189	1
3.1×10^5	93.8	700	775	3.9	388	100
4.1×10^3	51.3	780	2040	8.4	190	1000

Table 9
Real process: 2 independent reactions and fast heat transfer

$k_{01,1}$ in s^{-1}	$E_{1,1}$ in kJ mol^{-1}	$T_{max,1,real}$ in °C	$T_{max,1,nominal}$ in °C	$k_{01,2}$ in s^{-1}	$E_{1,2}$ in kJ mol^{-1}	$T_{max,2,real}$ in °C	$T_{max,2,nominal}$ in °C	U in J s^{-1} m^{-2} K^{-1}	Heating rate in °C s^{-1}
5×10^7	112.0	345	345	5×10^{17}	242.1	375	375	300	0.25
5×10^7	112.0	395	395	5×10^{17}	242.1	395	395	300	1
5×10^7	112.0	535	535	5×10^{17}	242.1	480	560	300	100
5×10^7	112.0	680	1240	5×10^{17}	242.1	520	1150	300	1000

Correlation model: 1 single reaction and extremely rapid heat transfer

k_{01} in s^{-1}	E_1 in kJ mol^{-1}	T_{max} in °C	$k_{1000\,K}$ in s^{-1}	Heating rate in °C s^{-1}
1.4×10^7	111.3	360	20.6	0.25
2.3×10^{10}	147.9	385	418.3	1
1.6×10^{10}	158.5	575	82.8	100
2.2×10^{10}	256.5	1190	8.4×10^{-4}	1000

Table 10
Real process: 2 independent reactions and slow heat transfer

$k_{01,1}$ in s^{-1}	$E_{1,1}$ in kJ mol^{-1}	$T_{max,1,real}$ in °C	$T_{max,1,nominal}$ in °C	$k_{01,2}$ in s^{-1}	$E_{1,2}$ in kJ mol^{-1}	$T_{max,2,real}$ in °C	$T_{max,2,nominal}$ in °C	U in J s^{-1} m^{-2} K^{-1}	Heating rate in °C s^{-1}
5×10^7	112.0	345	345	5×10^{17}	242.1	375	375	80	0.25
5×10^7	112.0	395	395	5×10^{17}	242.1	395	395	80	1
5×10^7	112.0	560	805	5×10^{17}	242.1	480	770	80	100
5×10^7	112.0	660	2090	5×10^{17}	242.1	510	1960	80	1000

Correlation model: 1 single reaction and extremely rapid heat transfer

k_{01} in s^{-1}	E_1 in kJ mol^{-1}	T_{max} in °C	$k_{1000\,K}$ in s^{-1}	Heating rate in °C s^{-1}
1.6×10^7	112.1	360	21.6	0.25
4.93×10^{10}	152.4	388	524.1	1
8.9×10^{13}	271.4	780	0.56	100
2.2×10^{11}	452.4	2020	4.67×10^{-13}	1000

range of lignocellulosic residues). This study attempts to show the causes of the differences between the kinetic parameters obtained from the TG and Pyroprobe data. Four cases have been analysed:

1. Two independent reactions where the heat transfer is extremely fast.
   1.1. Correlation model to a single reaction taking heat transfer into account.
   1.2. Correlation model to a single reaction without taking heat transfer into account.
2. Two independent reactions where the heat transfer is not fast.
   2.1. Correlation model to a single reaction taking heat transfer into account.
   2.2. Correlation model to a single reaction without taking heat transfer into account.

The expressions used to generate the theoretical data were similar to Eqs. (17) and (18) for two reactions

$$\frac{dW_i}{dt} = -k_{01,i} \exp(-E_{1,i}/RT)(W_i - W_{i,\infty}) \tag{19}$$

$$T_n = T_0 + \beta t \tag{20}$$

where T_n is the nominal temperature (K) and the subscript i refers to each one of the two independent reactions. When the heat transfer is considered extremely fast, T equals T_n.

When the heat transfer process was taken into account, two expressions similar to Eqs. (15) and (16) were considered, replacing T_t by T_n.

Simulated curves of weight loss vs. temperature are obtained by numeric integration by the fourth-order Runge–Kutta algorithm of Eqs. (15) and (19) together with Eqs. (16) and (20).

The kinetic parameter values used were: $k_{01,1} = 5 \times 10^7$ s^{-1}, $k_{01,2} = 5 \times 10^{17}$ s^{-1}, $E_{1,1}/R = 13\,500$ K, and $E_{1,2}/R = 29\,200$ K, corresponding to the decomposition processes of almond shells calculated by Font et al. [3].

Four heating rates (β), 0.25, 1, 100 and 1000°C s^{-1} and two heat transfer coefficients (U), 300 and 80 J s^{-1} m^{-2} K^{-1} were used to generate the curves. The other values considered were the following: $W_{ash} = 5\%$, $A = 2$ m^2 kg^{-1}, $W_{1,0} = W_{2,0} = (1 - 0.05)/2$ and $W_{1,\infty} = W_{2,\infty} = 0.15 \times W_{1,0}$.

Simulated data generated in this way were correlated with a model which considered a single decomposition process. The equations used were similar to Eqs. (15), (16), (19) and (20) for a single reaction. The Simplex Flexible Method [25] was used to optimise the activation energy of the process, the kinetic constant at 1000 K, and the value of the heat transfer coefficient.

Tables 5–10 show the cases analysed and the results obtained. In each case, kinetic parameters of the theoretical processes, heating rate, heat transfer coefficient used (when the heat transfer was considered) and approximate values of real and nominal T_{max} are shown (when heat transfer is fast, the nominal temperature coincides with the real temperature). In the case of the fitted process, the same parameters are presented together with the kinetic constant at 1000 K.

The results obtained show the following aspects:

Concerning the single reaction:

1. From Tables 5, 7 and 8 it can be deduced that at 1000°C s^{-1}, T_{max} values for process 1 are 640, 680 and 660°C when the U value is ∞, 300 and 80, respectively. The presence of a maximum value of T_{max}, instead of increasing or decreasing monotonically as expected, is due to the assumed variation of C_{p_B} with the composition of ash, because if C_p is considered constant throughout the process the maximum disappears. This demonstrates the importance of considering the C_p dependence on time when these processes are simulated.

2. Again, the shift of the peaks to high temperatures when the heating rate is increased is observed. In these cases, reaction 1 is more sensitive to the heating rate

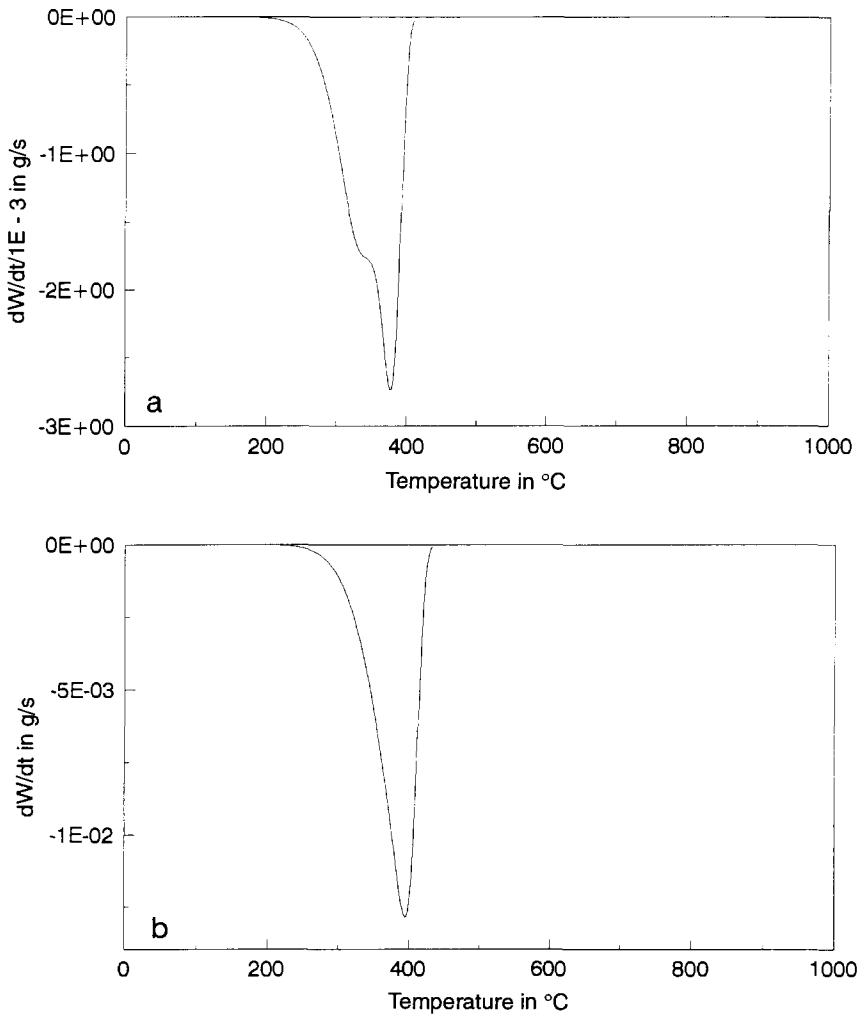

Fig. 5(a) and (b)

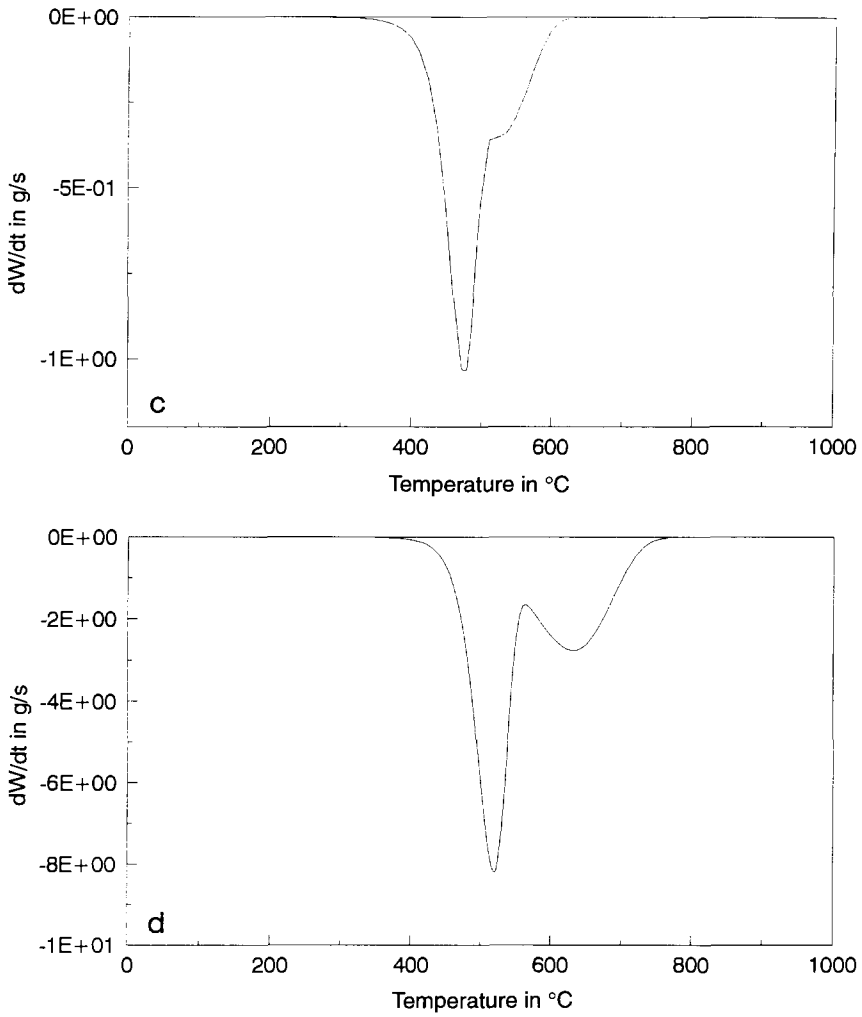

Fig. 5. Simulation of weight loss vs. temperature for two independent reactions at different heating rates: (a) 0.25°C s^{-1}; (b) 1°C s^{-1}; (c) 100°C s^{-1}; (d) 1000°C s^{-1}.

than process 2, so although process 1 takes place at lower temperatures than reaction 2 at 0.25°C s^{-1}, the appearance order is inverted at 100°C s^{-1} and both processes overlap at 1°C s^{-1}. Fig. 5 shows this fact (two independent reactions and heat transfer extremely fast, see Tables 5 and 6).

3. When the heat transfer is not fast, a difference between the real and nominal temperatures is observed. Obviously, this difference increases when the heating rate increases.

Concerning the correlation:

4. Four cases are distinguished:

4(a) In the generating model and in the correlation model, the heat transfer is considered very fast (Table 5).

4(b) In the generating model, the heat transfer is very fast but in the correlation model, the heat transfer considered is not fast (Table 6).

4(c) In the generating model and in the correlation model, the heat transfer is not very fast (Tables 7 and 8).

4(d) In the generating model, the heat transfer is not very fast, but in the correlation model, an extremely fast heat transfer is considered (Tables 9 and 10).

In cases 4(a), 4(b) and 4(c), the values of the activation energy obtained were always lower than the highest values of the original reactions [34,35]. Because the activation energy is related to the peak width, when two processes are fitted by a single reaction the activation energy value obtained depends on the distance between the peaks: when both reactions take place at different ranges of temperature, a low activation energy fits better. As both peaks approach, the overall range of temperatures decreases; therefore, the activation energy of the fitted reaction increases. When process 1 has overtaken process 2 and the distance between them is again increased, the activation energy value decreases. A maximum value of the activation energy is shown when both peaks are superposed. Pre-exponential factor and kinetic constant values follow the same trend.

The heat transfer coefficient obtained in the correlation has no significant value when the process is performed at low heating rates because the gap between actual and nominal temperature is not important. When this difference is great (at high heating rates), the heat transfer coefficient obtained has a significant value and this coefficient is always higher than the real one.

Note that the only difference between Tables 5 and 6 is the inclusion of the heat transfer term in the correlation model although it was not included in the data generation. In these cases, the kinetic parameters obtained as well as the T_{max} values are very similar. This is logical because both cases turn into the same by fitting U at very high values, which means an extremely fast heat transfer ($U = 24\,000$ and $98\,000$ J s^{-1} m^{-2} K^{-1} when the values of the heating rate are high, Table 6).

In case 4(d) (Tables 9 and 10), the trend of the fitted parameters is different. In these tables, the theoretical data generated include the heat transfer term but this was not taken into account in the correlation model, which considers the nominal temperature as the real temperature of the reaction. The activation energy obtained is therefore an apparent value because the difference between actual and nominal temperatures is important at high heating rates. This value follows an increasing trend when the heating rate increases, because the nominal temperatures are significantly increased at high heating rates. This trend is logically more marked in the case where the heat transfer of the real processes is slower ($U = 80$ J s^{-1} m^{-2} K^{-1}). The kinetic constants show a maximum and their values decrease remarkably at high heating rates.

When data generated from a multiple process are correlated by a model which considers a single reaction, the kinetic parameters obtained differ from the real ones and the difference increases when the difference between the nominal and real

temperatures increases. Taking into account that the value of T_{max} depends on the heating rate, the differences are logical between the kinetic parameters obtained by correlating TG data (heating rate is in the range 1.5–200°C min^{-1}), according to the two reactions model, and Pyroprobe data (heating rate around 300°C s^{-1}, nominal heating rate = 20 000°C s^{-1}), using a single reaction model.

4. Conclusions

From the study on MSW thermogravimetric analysis, the following conclusions can be deduced:

1. For each TG experiment, the weight loss of MSW as a function of temperature cannot be simulated by considering a single decomposition reaction.
2. For each TG experiment, the weight loss of MSW as a function of temperature can be simulated by considering that the overall process is formed by two independent reactions: (a) decomposition, around 310–380°C at 1.5–200°C min^{-1}, of the cellulosic fraction, and (b) decomposition of the other fraction in the range 200–500°C.
3. When the heat transfer between the sample and its surroundings was considered in the model proposed, the dispersion of the results was not reduced. This shows that the dispersion is due more to the sample heterogeneity than to an important gap between the actual temperature and that measured by the thermocouple.
4. The mean values of the kinetic parameters obtained for both decomposition reactions were: $k_{01,C} = 2.92 \times 10^9$ s^{-1}, $k_{02,NC} = 1.13$ s^{-1}, $E_{1,C} = 135.9$ kJ mol^{-1}, and $E_{1,NC} = 26.8$ kJ mol^{-1}.
5. The dispersion of the kinetic constant of the first process (cellulosic fraction decomposition) is lower than the constant of the second process (decomposition of the other organic refuses), which is logical taking into account the MSW composition.

From the simulation carried out with a system with two reactions, it can be concluded that:

6. If data generated from a multiple process are correlated by a model which considers a single reaction, the kinetic parameters obtained will differ from the real ones and this difference increases when the difference between the real and nominal temperature increases.
7. The sample heat capacity varies with time and this fact influences the appearance of the TG peaks.

Acknowledgement

Support for this work was provided by CICYT-Spain, Research project AMB93-1209.

References

[1] K.A. Agrawal, Compositional Analysis of Solid Waste and Refuse Derived Fuels by Thermogravimetry, Compositional Analysis by Thermogravimetry, ASTM STP 997, C.M. Earnest (Ed.), American Society for Testing and Materials, Philadelphia, 1988, p. 259.
[2] S.S. Alves and J.L. Figueiredo, J. Anal. Appl. Pyrol., 13 (1988) 123.
[3] R. Font, A. Marcilla, E. Verdú and J. Devesa, J. Anal. Appl. Pyrol., 21 (1991) 249.
[4] G. Varhegyi, M.J. Antal, Jr., T. Szekely and P. Szabo, Energy & Fuels, 3 (1989) 329.
[5] T. Cordero, F. García and J.J. Rodríguez, Thermochim. Acta, 149 (1989) 225.
[6] T. Cordero, J.M. Rodríguez-Maroto, J. Rodríguez-Mirasol and J.J. Rodríguez, Thermochim. Acta, 164 (1990) 135.
[7] R. Bilbao, J. Arauzo and A. Millera, Thermochim. Acta, 120 (1987) 121.
[8] R. Bilbao, J. Arauzo and A. Millera, Thermochim. Acta, 120 (1987) 133.
[9] M.J. Antal, Jr., W.S.L. Mok, J.C. Roy and A. T-Raissi, J. Anal. Appl. Pyrol., 8 (1985) 291.
[10] D.L. Urban and M.J. Antal, Jr., Fuel, 61 (1982) 799.
[11] W.S.-L. Mok and M.J. Antal, Jr., Thermochim. Acta, 68 (1983) 165.
[12] D.Q. Tran and C. Rai, AIChE Symp. Ser., 75 (1979) 41.
[13] H.E. Kissinger, Anal. Chem., 29 (1957) 1702.
[14] D. Chen, X. Gao and D. Dollimore, Thermochim. Acta, 215 (1993) 109.
[15] D. Chen, X. Gao and D. Dollimore, Thermochim. Acta, 215 (1993) 65.
[16] T. Cordero, J.M. Rodríguez-Maroto, J.M. García and J.J. Rodríguez, Thermochim. Acta, 191 (1991) 161.
[17] R. Font, A. Marcilla, J. Devesa and E. Verdú, Ind. Eng. Chem. Res., 27 (1988) 1143.
[18] R. Font, A. Marcilla and J. Devesa, Ind. Eng. Chem. Res., 29 (1990) 1846.
[19] A.N. García, R. Font and A. Marcilla, J. Anal. Appl. Pyrol., 23 (1992) 99.
[20] J.A. Caballero, R. Font, A. Marcilla and A.N. García, J. Anal. Appl. Pyrol., 27 (1993) 221.
[21] E. Gutiérrez Ríos, Química Inorgánica, Reverté, Barcelona, 1985.
[22] C.J. Keattch and D. Dollimore, An Introduction to Thermogravimetry, Heyden, London, 1975.
[23] W.W. Wendlandt, Thermal Analysis, Chemical Analysis, Vol. 19, Wiley, New York, 1986.
[24] P. Raman, W.P. Walawender, L.T. Fan and J.A. Howel, Ind. Eng. Chem. Process Des. Dev., 20 (1981) 630.
[25] D.M. Himmelblau, Process Analysis Statistical Methods, Wiley, New York, 1970.
[26] J.E. Helt, R.F. Henry and J.W. Young, Energy Munic. Waste Res., (1984) 59.
[27] R.H. Perry and C.H. Chilton, Chemical Engineers' Handbook, McGraw-Hill, Kogakusha, Tokyo, 1973.
[28] U. Biader Ceipidor, R. Bucci and A.D. Magrí, Thermochim. Acta, 161 (1990) 37.
[29] R.H. Borgwardt, AIChE J., 31 (1985) 103.
[30] K. Akita and M. Kase, J. Polym. Sci. Part A1, 5 (1967) 833.
[31] M. Antal, Jr., H.L. Friedman and F.E. Rogers, Combust. Sci. Technol., 21 (1980) 141.
[32] J.H. Flynn, Thermochim. Acta, 37 (1980) 225.
[33] J.H. Flynn, J. Polym. Sci., 20 (1980) 675.
[34] H. Juntgen and K.H. Van Heek, Reacktionablaufe unter nichtisothermen Bedingungen, Fortschritte der chemischen Forschung, 13, Springer-Verlag, Berlin, 601, 1970; trans., Belov and Assoc., Denver, CO, APTIC-TR-0776.
[35] J.B. Howard, Fundamentals of Coal Pyrolysis and Hydropyrolysis, Chemistry of Coal Utilization, Wiley, New York, 1981.